0026-895X/95/061078-09$3.00/0

MOLECULAR PHARMACOLOGY, 48:1078–1086 (1995).

Mechanism of Cytochrome P450 2D6-Catalyzed Sparteine Metabolism in Humans

THOMAS EBNER,[1] CLAUS O. MEESE,[2] and MICHEL EICHELBAUM

Dr. Margarete Fischer-Bosch-Institut für Klinische Pharmakologie, D-70376 Stuttgart, Germany

Received June 12, 1995; Accepted September 5, 1995

SUMMARY

Two different reaction mechanisms for the formation of the two human enamine-structured sparteine metabolites by cytochrome P450 2D6 have been discussed in the literature. These mechanisms are either initial one-electron oxidation of N1 of sparteine followed by deprotonation of the aminium radical cation, resulting in the formation of different carbon radicals and oxygen rebound of the carbon radicals, or oxidation of the carbon atoms adjacent to N1 by the enzyme, directly producing the respective carbon radicals. With a spectrum of deuterium-labeled isotopomers of sparteine, stereoselectivity and kinetic isotope effects of human sparteine metabolism were investigated by *in vitro* and *in vivo* experiments and were compared with chemical oxidation of 17-oxosparteine. These experiments revealed that the major human sparteine metabolite 2,3-didehydrosparteine is formed via highly stereoselective abstraction of the 2β-hydrogen atom; the deuterium label was completely retained during metabolism when 2*R*-[^{2}H]sparteine was used as substrate. Chemical oxidation of 17-oxosparteine by Ce^{4+}, as a model for one-electron oxidation of N1 of a sparteine-like structure, resulted in the sole formation of the 5,6-unsaturated enamine, and no 2,3-unsaturated enamine, structurally equivalent to the human major metabolite, was found. An unequivocal discrimination between the two possible reaction mechanisms was not possible by simple interpretation of the magnitude of the kinetic deuterium isotope effects. However, results of competitive and noncompetitive experiments revealed the presence of a nondissociative enzymatic mechanism for the formation of the two sparteine metabolites, i.e., the sparteine molecule that is bound to the substrate binding site of cytochrome P450 2D6 performs orientational changes without dissociating from the activated enzyme/substrate complex before the product-determining first irreversible reaction step. These results agree with the hypothesis that sparteine metabolism proceeds by direct carbon oxidation. Because electron transfer from amines to P450 may occur over some distance, the possibility of a sequential electron-proton transfer reaction during sparteine metabolism cannot be ruled out completely as an alternative reaction mechanism for sparteine metabolism.

The oxidative metabolism of sparteine (**1**), a quinolizidine alkaloid with antiarrhythmic properties, is catalyzed by human CYP2D6 and therefore exhibits a genetic polymorphism. Of whites, 5–10% have a severely impaired capacity to metabolize sparteine and eliminate most of the dose as parent drug in the urine. These individuals are therefore designated as poor metabolizers, whereas the majority of the white and non-white population is defined as EMs because they eliminate most of the drug as metabolites. Although sparteine is no longer in therapeutic use, it is still a useful model and probe drug for polymorphic drug metabolism by CYP2D6.

Two enamine-structured sparteine derivatives, 2,3-didehydrosparteine (**2**) and 5,6-didehydrosparteine (**3**), are detected by GC-MS as the major human metabolites in urine or plasma samples of EMs (Fig. 1). The same metabolites are also found in *in vitro* experiments using EM human liver microsomes. However, these enamines constitute rearrangement or decomposition products due to alkaline sample work-up and extraction before GC-MS analysis. It could be shown by NMR analysis that at neutral pH, the major metabolite 2,3-didehydrosparteine is present almost exclusively as the hydrated form 2*S*-hydroxysparteine (**4**), whereas 5,6-didehydrosparteine is present as the tautomeric 1,6-unsaturated iminium ion (**5**).[3]

Because CYP2D6 exhibits a distinct substrate specificity (3), refined models of its substrate binding site have been developed (4–6). Typical CYP2D6 substrates possess a basic nitrogen atom that interacts with a negatively charged functional group in the CYP2D6 substrate binding site and are metabolically attacked at a distance of 4.5–8 Å (4) from the

This work was supported by the Robert-Bosch-Stiftung, Stuttgart, Germany.

[1] Current affiliation: Dr. Karl Thomae GmbH, Department of Pharmacokinetics and Drug Metabolism, D-88397 Biberach, Germany.

[2] Current affiliation: Schwarz Pharma AG, Synthesis and Isotope Laboratory, D-40789 Monheim, Germany.

[3] During the present study, the sparteine metabolites were detected and quantified as free enamine bases, i.e., **2** and **3**; therefore, these designations were used instead of **4** and **5**.

ABBREVIATIONS: CYP2D6, cytochrome P450 2D6; P450, cytochrome P450; EM, extensive metabolizer; EOS, activated cytochrome P450 (enzyme) substrate complex; GC, gas chromatography; MS, mass spectrometry.

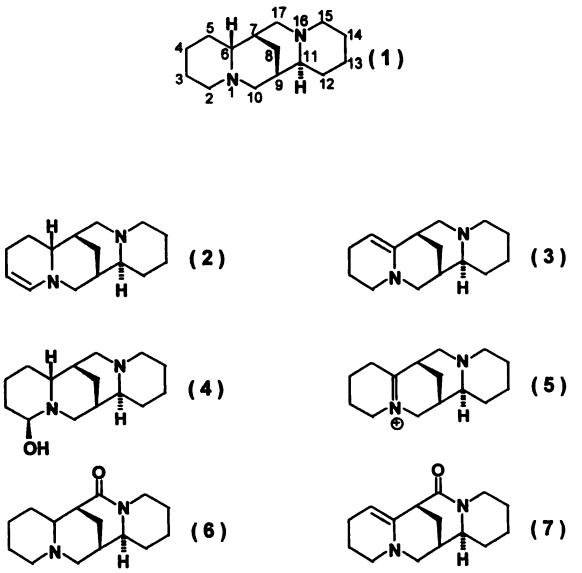

Fig. 1. Structures of sparteine, sparteine metabolites, and oxosparteine derivatives that were used for chemical oxidation experiments. The enamine structured human major metabolites 2,3-didehydrosparteine (**2**) and 5,6-didehydrosparteine (**3**) are monitored after alkaline extraction by GC or GC-MS.

basic nitrogen atom. Unlike many other substrates of CYP2D6, sparteine has a rigid structure with no flexible side chains and adopts a protonated all-chair configuration when dissolved in aqueous medium of neutral pH (7). Additional information on regioselectivity and stereoselectivity of sparteine metabolism would therefore facilitate modeling of the active binding site of CYP2D6. On the other hand, the mechanism resulting in the formation of sparteine metabolites should match the structural requirements of the CYP2D6 substrate binding site. However, the mechanism of CYP2D6-catalyzed sparteine metabolism remains unclear.

Two potential reaction mechanisms for the formation of the human sparteine metabolites are displayed in Fig. 2. Briefly, mechanism A proceeds via initial enzymatic one-electron oxidation of N1 followed by deprotonation of the aminium radical cation and oxygen rebound of the respective carbon radicals (8). According to mechanism B, the different carbon radicals are formed by direct hydrogen atom abstraction.

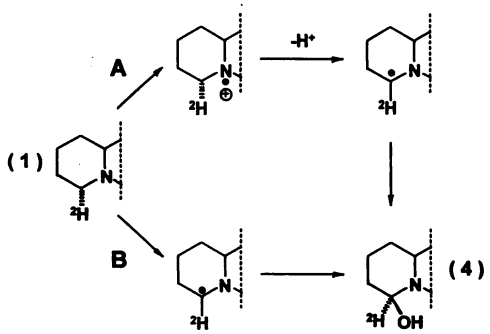

Fig. 2. Possible mechanisms of sparteine metabolite formation by CYP2D6. Formation of 2-[^{2}H]-**4** from 2*R*-[^{2}H]-**1** is shown. Mechanism A (postabstraction mechanism): Initial one-electron oxidation of N1 leading to the aminium radical cation followed by proton abstraction and formation of a carbon-centered radical; oxygen rebound finally leads to the formation of 2-[^{2}H]-**4**. Mechanism B (preabstraction mechanism): Direct carbon oxidation by CYP2D6 followed by oxygen rebound.

Both mechanisms produce the carbinolamine-structured 2- or 6-hydroxy sparteines.

It has been reported that oxidative attack of the N1 nitrogen atom of the sparteine molecule appears to not be consistent with the molecular template of CYP2D6 substrates (4). Therefore, extensive investigations on the reaction mechanism of the formation of the human sparteine metabolites were performed during the present study, including *in vitro* and *in vivo* experiments with a spectrum of regiospecifically and stereospecifically deuterated analogues of **1**. Because stereoselective hydrogen abstraction occurs during the formation of **2** in rats (9), GC-MS was used to assess stereoselectivity of human sparteine metabolism. Kinetic deuterium isotope effects associated with the formation of sparteine metabolites were also measured because kinetic isotope effects have been a valuable tool for the study of the reaction mechanisms of a variety of P450-catalyzed heteroatom oxidation reactions, such as aliphatic or aromatic *N*-dealkylations (10, 11). To further investigate the kinetic mechanisms of human sparteine metabolism, we used an experimental approach described by Gillette *et al.* (12, 13) that involves competitive and noncompetitive experiments with selectively deuterated substrates. In this context, competitive means that a mixture of two differently deuterated isotopomers of the same compound are used as substrate, whereas in noncompetitive experiments single isotopomers are used.

In addition, chemical oxidation of sparteine and 17-oxosparteine was examined and compared with enzymatic metabolism with respect to product formation and deuterium isotope effects.

Materials and Methods

Chemicals. 2*R*-[^{2}H]-**1**, 2*S*-[^{2}H]-**1**, 2,2-[$^2H_2$]-**1**, 5,5-[$^2H_2$]-**1**, and 6-[^{2}H]-**1** were obtained as described previously (14–17). 15,15,17,17-[$^2H_4$]-**1** was synthesized starting from 15-oxosparteine via 15,15-[$^2H_2$]-**1** and 15,15-[$^2H_2$]-17-oxosparteine, as described below. Undeuterated **1**-sulfate was obtained (Aldrich Chemical Co., Steinheim, FRG) from which the free base was liberated and purified by vacuum distillation. Stable, crystalline **1**-sulfates × 5 H_2O were prepared from freshly distilled sparteine isotopomer bases (16) and used for *in vitro* and *in vivo* experiments. 17-Oxosparteine (**6**), 15-oxosparteine, 5,6-didehydro-17-oxosparteine (**7**), 17-ethylsparteine, 2,3-didehydrosparteine (**2**), and 5,6-didehydrosparteine (**3**) were synthesized according to published procedures (18–20). NADPH was purchased from Sigma Chemical Co. (Steinheim, FRG); all other reagent-grade chemicals were obtained from Merck (Darmstadt, FRG) or Aldrich.

Syntheses. 15,15-[$^2H_2$]-**1** and 15,15,17,17-[$^2H_4$]-**1** were synthesized by lithium aluminum deuteride reduction of 15-oxosparteine or 15,15-[$^2H_2$]-**6**, respectively, in the following manner. A solution of 12.5 mmol of the corresponding oxosparteine in 15 ml of absolute tetrahydrofuran was slowly (over 10 min) added to a stirred suspension of 19 mmol of $LiAl^2H_4$ in absolute tetrahydrofuran under argon at room temperature. The mixture was refluxed for 30 min, and the crude product was isolated by quenching the reaction with 5 ml of water (0°) and 10 ml of 20% (w/v) KOH followed by extraction with diethyl ether. The combined organic phases were dried over Na_2SO_4, and the solvent was evaporated under reduced pressure. The resulting oil was dissolved in 50 ml of dry ethanol, and the solution was neutralized by the addition of 60% (w/v) perchloric acid. Iminium-structured side products of $LiAl^2H_4$ reduction, which were present in the crude product, were reduced by the addition of 15 mmol of sodium borodeuteride with constant stirring at room temperature. The reaction mixture was maintained at room temperature for 30

min, followed by evaporation of the solvent and the addition of 20 ml 20% KOH. The crude sparteine base was extracted with diethyl ether and subjected to distillation under reduced pressure (105–110°, 0.04–0.1 mbar). Pure sparteine bases were obtained in 78–91% yield. ^{13}C NMR (300 MHz, $C_6{}^2H_6$, internal standard tetramethylsilane) proved complete deuterium labeling at C15 and C17, respectively (unlabeled **1**: 55.78 ppm [C15], 54.00 ppm [C17]; Ref. 19).

Crystalline monohydrogen sulfate pentahydrates were obtained from the distilled bases 15,15-[$^2H_2$]-**1**: m.p. 138°; calculated for $C_{15}H_{24}{}^2H_2N_2 \times H_2SO_4 \times 5\ H_2O$: C 42.44%, H + ^2H, 9.50%, N 6.59%, S 7.55%; found: C 42.38%, H + ^2H 9.69%, N 6.50%, S 7.65%; and 15,15,17,17-[$^2H_4$]-**1**: m.p. 139°; calculated for $C_{15}H_{22}{}^2H_4N_2 \times H_2SO_4 \times 5\ H_2O$: C 42.34%, H + ^2H 9.71%, N 6.58%, S 7.53%; found: C 42.39%, H + ^2H 9.74%, N 6.59%, S 7.50%. 15,15-[$^2H_2$]-**6** and 6-[^2H]-**6** were prepared by hexacyanoferrate oxidation of 15,15-[$^2H_2$]-**1** or 6-[^2H]-**1**, respectively. Of the corresponding sparteine base, 16.3 mmol was dissolved in 70 ml of 0.4 M HCl. After the addition of 105 ml of 10% (w/v) NaOH, the resulting emulsion was immediately mixed with 90 ml of an aqueous solution of 70 mmol of $K_3[Fe(CN)_6]$ at room temperature. The reaction mixture was vigorously shaken for 10 min, made strongly alkaline by the addition of 20% (w/v) NaOH, and extracted with diethyl ether (five times, 100 ml). The combined ether solutions were dried (Na_2SO_4), and the solvent was removed under reduced pressure. The remaining oil was dissolved in 10 ml of hexane. The crystalline product was recrystallized twice from the same solvent, 15,15-[$^2H_2$]-**6**: m.p. 84°; calculated for $C_{15}H_{22}{}^2H_2N_2O$: C 71.95%, H + ^2H 10.47%, N 11.19%; found C 72.12%, H + ^2H 10.63%, N 11.04%. 6-[^2H]-**6**: m.p. 85°; calculated for $C_{15}H_{23}{}^2HN_2O$: C 72.25%, H + ^2H 10.11, N 11.23%; found: C 72.33, H + ^2H 10.11%, N 11.13%.

Human liver microsomes. Samples of human livers (from kidney donors) were generous gifts of Prof. U. A. Meyer, Basel, Switzerland. Liver samples were assigned to the EM phenotype on the basis of genotyping (*XbaI* restriction fragment length polymorphism and polymerase chain reaction analyses) and enzyme kinetic studies of CYP2D6-catalyzed **1** and bufuralol metabolism. Microsomes of liver samples were prepared as described previously (21).

***In vitro* experiments with human liver microsomes.** Incubations with human liver microsomes were performed as described previously (22). Briefly, 50 μg of microsomal protein was incubated for 40 min at 37° in a total volume of 250 μl of 100 mM Tris·HCl buffer, pH 7.5, in presence of 6 mM $MgCl_2$ and 4.8 mM NADPH. For competitive experiments, mixtures of tetradeuterated 15,15,17,17-[$^2H_4$]-**1** sulfate and either [$^2H_0$]-**1**, 2*R*-[^2H]-**1**, 2*S*-[^2H]-**1**, 2,2-[$^2H_2$]-**1**, or 6-[^2H]-**1** sulfates were prepared in equimolar ratio, which was subsequently verified by GC-MS analysis. These 50:50 mixtures were used for *in vitro* experiments at final concentrations of 40, 80, and 160 μM. Reaction was stopped by the addition of 10 μl 60% (w/v) perchloric acid, and the mixtures were stored frozen (−20°) until use. After the addition of internal standard (17-ethylsparteine), samples were made strongly alkaline (50 μl of 12.5 M NaOH solution) and subsequently extracted with 50 μl of dichloromethane (through vortexing). After centrifugation (5 min at 6000 × *g*), 1 μl of the clear organic phase was directly injected onto the capillary column. In noncompetitive experiments, substrate concentrations were 10, 20, 40, 80, 160, and 320 μM.

GC and GC-MS analyses. For incubations with single isotopomers of **1**, GC analysis was performed as described (22) on a Carlo Erba Fractovap 4160 with cooled on-column injection and nitrogen/phosphorus selective detection. GC-MS analysis of incubation experiments with equimolar mixtures of 15,15,17,17-[$^2H_4$]-**1** and differently labeled sparteines was done with a Hewlett-Packard HP5790 MSD using electron impact (70 eV) ionization coupled with an HP5890 gas chromatograph. Incubations of **6** with human liver microsomes followed the protocol for the incubation of **1** described above.

***In vivo* experiments.** Fifty milligrams of equimolar mixtures of sulfates of 15,15,17,17-[$^2H_4$]-**1** and differently labeled sparteines ([$^2H_0$]-**1**, 2*R*-[^2H]-**1**, 2*S*-[^2H]-**1**, 6-[^2H]-**1**) dissolved in 100 ml of water were orally administered to a healthy volunteer who had been previously phenotyped as EM. Urine was collected in five 3-hr fractions for 15 hr and was stored frozen (−20°) until GC or GC-MS analysis. Sample work-up and quantification of sparteine metabolites were performed according to the published procedure (22a).

Chemical oxidation of 17-oxosparteine. Equimolar mixtures of either [$^2H_0$]-**6** and 15,15-[$^2H_2$]-**6** or 6-[^2H]-**6** and 15,15-[$^2H_2$]-**6** were dissolved in acetonitrile (5 mM) and used for chemical oxidation experiments. A saturated solution of ammonium cer-IV-nitrate in acetonitrile was added in aliquots of 10 μl to 0.5 ml of the 17-oxosparteine solutions. The addition of cer-IV-nitrate was stopped when the reaction mixture remained yellow for 1 hr at room temperature. White precipitates developing after the addition of the first two aliquots of ammonium cer-IV-nitrate solution were dissolved by the addition of 10 μl of a solution of 1% (v/v) acetic acid and 4% (v/v) water in acetonitrile. For sample work-up, 25 μl of the clear reaction mixture was diluted with 0.3 ml of water. A solution of 50 μl 12.5 M NaOH and 50 μl of dichloromethane was then added. After centrifugation as described above, 1 μl of the dichloromethane phase was used for GC-MS analysis. A modified temperature program, which included a final 20-min period at 270°, was used for experiments with 17-oxosparteine to ensure the detection of products with longer retention times. Deuterium isotope effects were calculated by direct comparison of the relative amounts of the formed product isotopomers by quantification of the quasimolecular ions of 15,15-[$^2H_2$]-**7** (m/z = 248.1) and unlabeled **7** (m/z = 246.1).

Other assays. Protein concentrations were determined by the Lowry method. Isotopic composition of the deuterated sparteines was determined by GC-MS using selected ion monitoring of the molecular cluster ion (M + 1) and chemical ionization (reactant gas NH_3). An HP5985A mass spectrometer, operated in positive-ion chemical ionization mode (72 eV), coupled to an HP5890 gas chromatograph was used for GC and MS measurements. Deuterium content was >96% of the stated isotopic composition of the differently labeled sparteines. Regioselectivity and stereoselectivity of the deuterium labeling were verified by ^{13}C or ^2H NMR spectroscopy for all deuterated sparteine isotopomers.

Calculation of isotope effects. *In vitro* kinetic isotope effects were measured by competitive and noncompetitive methods (23). The ratio between the rates of metabolism of the two differently labeled sparteines was measured for the competitive method by GC-MS. For this purpose, GC-MS tracings of m/z = 232.4 (for unlabeled didehydro metabolites) or m/z = 233.4 (for [$^2H_1$]didehydro metabolites) were recorded by selected ion monitoring. The respective peak areas were compared with the peak area of the simultaneously recorded mass tracing of the [$^2H_4$]didehydro metabolites at m/z = 236.4. Because substrate conversion in *in vitro* experiments was small (<5%), the apparent isotope effect, ^{D}(V/K), could be estimated from the ratio between the tetradeuterated metabolites and the metabolites that were formed from the **1** isotopomers labeled at positions 2 or 6 (23, 24). In the noncompetitive method, the rates of metabolism of differently labeled sparteines were measured separately. Enzyme kinetic parameters, V_{max} and K_m, were estimated using a nonlinear regression program (Enzfitter, Biosoft, Cambridge, UK). For *in vivo* studies, relative amounts (expressed as percentage of dose) of the excreted metabolite were used for the noncompetitive design after the administration of single **1** isotopomers. GC-MS analysis was used for the competitive design according to the procedure for *in vitro* experiments.

Molecular modeling. Simple molecular modeling of sparteine was done using the program Alchemy II (Tripos Associates).

Statistical analysis. Statistical analysis was performed using Student's *t* test; values of $p < 0.05$ was considered to be statistically significant.

Results

Noncompetitive enzyme kinetic studies on sparteine metabolism and stereoselectivity of deuterium abstraction. Incubations of different **1** isotopomers resulted in the formation of the two human metabolites that followed monophasic Michaelis-Menten kinetics. Enzyme kinetic parameters found in noncompetitive *in vitro* experiments are listed in Table 1. Deuterium substitutions did not result in significant changes to K_m values, but V_{max} values for the formation of **2** and **3** were clearly reduced when the substrate was labeled in positions 2*S* or 6, respectively. As expected, **3** formed from 6-[^{2}H]-**1** showed a complete loss of the deuterium label. In contrast, deuterium was abstracted in the course of **2** formation only when 2*S*-[^{2}H]-**1** was used as substrate but was retained to >95% in **2** formed from 2*R*-[^{2}H]-**1**. No kinetic isotope effect was observed when 5,5-[$^2H_2$]-**1** was used as substrate. GC-MS measurements revealed a complete loss of both deuterium atoms in **3** formed from 5,5-

TABLE 1

Kinetic deuterium isotope effects for *in vitro* sparteine metabolism determined by noncompetitive experiments

Incubations and analyses were performed as described in Materials and Methods. Values from computerized nonlinear regression analysis ± standard error of estimate. Mean values of three separate experiments were used for computerized calculation of V_{max} and K_m. *V/K* denotes the ratio of V_{max}/K_m as a measure of the intrinsic enzyme activity at low, nonsaturating substrate concentrations.

Liver sample	Substrate	2,3-Didehydrosparteine			
		K_m	V_{max}	$D_{(V/K)}$[a]	KIE[b]
		μM	pmol/min/mg		
1	[$^2H_0$]-1	56.7 ± 7.1	323 ± 13.9	1.00	1.00
	15,15,17,17-[$^2H_4$]-1	56.9 ± 9.5	324 ± 18.7	1.00	0.97
	2*R*-[^{2}H]-1	53.1 ± 6.9	306 ± 13.6	0.99	1.01
	2*S*-[^{2}H]-1	52.1 ± 9.0	141 ± 8.3	2.10	2.99
	2,2-[$^2H_2$]-1	56.3 ± 11.2	144 ± 9.9	2.23	2.93
	6-[^{2}H]-1	52.2 ± 8.7	365 ± 20.7	0.81	0.30
	5,5-[$^2H_2$]-1	57.6 ± 4.6	325 ± 9.0	1.01	0.95
2	[$^2H_0$]-1	97.7 ± 9.7	203 ± 8.3	1.00	1.00
	15,15,17,17-[$^2H_4$]-1	99.1 ± 10.3	201 ± 8.6	1.02	0.98
	2*R*-[^{2}H]-1	99.3 ± 13.9	189 ± 14.7	1.09	1.11
	2*S*-[^{2}H]-1	97.1 ± 6.2	90.1 ± 3.9	2.24	3.44
	2,2-[$^2H_2$]-1	97.2 ± 10.9	94.9 ± 3.5	2.13	3.65
	6-[^{2}H]-1	100.4 ± 7.9	227 ± 7.4	0.92	0.31
	5,5-[$^2H_2$]-1	98.3 ± 8.4	204 ± 8.9	1.00	0.99
		5,6-Didehydrosparteine			
1	[$^2H_0$]-1	59.0 ± 6.9	125 ± 5.2	1.00	1.00
	15,15,17,17-[$^2H_4$]-1	57.6 ± 10.3	121 ± 7.7	1.01	1.04
	2*R*-[^{2}H]-1	57.2 ± 7.9	119 ± 5.7	1.02	1.00
	2*S*-[^{2}H]-1	55.2 ± 9.4	164 ± 9.7	0.71	0.33
	2,2-[$^2H_2$]-1	49.6 ± 7.7	164 ± 8.5	0.64	0.34
	6-[^{2}H]-1	58.9 ± 7.6	42.0 ± 1.9	2.97	3.32
	5,5-[$^2H_2$]-1	59.8 ± 5.6	120 ± 5.3	1.06	1.05
2	[$^2H_0$]-1	98.2 ± 8.3	70.5 ± 2.5	1.00	1.11
	15,15,17,17-[$^2H_4$]-1	96.2 ± 15.5	68.7 ± 4.5	1.01	1.12
	2*R*-[^{2}H]-1	99.8 ± 8.9	72.8 ± 2.7	0.98	1.00
	2*S*-[^{2}H]-1	96.2 ± 7.0	109 ± 2.8	0.63	0.32
	2,2-[$^2H_2$]-1	95.3 ± 14.7	122 ± 6.2	0.56	0.30
	6-[^{2}H]-1	99.5 ± 12.8	23.8 ± 2.4	3.00	3.54
	5,5-[$^2H_2$]-1	98.3 ± 11.3	70.0 ± 3.1	1.01	1.12
		Total metabolism			
		V/K (2) + *V/K* (3)	$D_{[V/K\ (2)\ +\ V/K\ (3)]}$		
1	[$^2H_0$]-1	7.82	1.00		
	15,15,17,17-[$^2H_4$]-1	7.79	1.00		
	2*R*-[^{2}H]-1	7.84	1.00		
	2*S*-[^{2}H]-1	5.68	1.38		
	2,2-[$^2H_2$]-1	5.86	1.33		
	6-[^{2}H]-1	7.71	1.01		
	5,5-[$^2H_2$]-1	7.65	1.02		
2	[$^2H_0$]-1	2.80	1.00		
	15,15,17,17-[$^2H_4$]-1	2.74	1.02		
	2*R*-[^{2}H]-1	2.63	1.06		
	2*S*-[^{2}H]-1	2.06	1.36		
	2,2-[$^2H_2$]-1	2.26	1.24		
	6-[^{2}H]-1	2.50	1.12		
	5,5-[$^2H_2$]-1	2.79	1.00		

[a] $D_{(V/K)}$, i.e., the apparent kinetic isotope effects in noncompetitive experiments were calculated from $(V_{max}/K_m)_H/(V_{max}/K_m)_D$.
[b] KIE values were calculated according to Ref. 12 from $[(v_{pw})_H/(v_{px})_H]/[(v_{pw})_D/(v_{px})_D]$.

TABLE 2

Kinetic deuterium isotope effects for *in vitro* sparteine metabolism determined by competitive experiments

Isotope effects were calculated from relative amounts of metabolites formed from equimolar mixtures of the differently labeled 1 isotopomers listed in the table together with 15,15,17,17-[$^2H_4$]-1 as described in Materials and Methods. Values are mean ± standard deviation from six experiments.

Product ratio	Deuterium-labeled sparteines				
	[$^2H_0$]-1	2*R*-[^{2}H]-1	2*S*-[^{2}H]-1	2,2-[$^2H_2$]-1	6-[^{2}H]-1
Liver sample 1					
$(3)_H/(3)_D$	1.02 ± 0.19	0.95 ± 0.10	0.64 ± 0.05	0.59 ± 0.04	2.31 ± 0.05
$(2)_H/(2)_D$	0.92 ± 0.08	0.94 ± 0.04	1.75 ± 0.08	1.75 ± 0.06	0.79 ± 0.03
$(2)_H/(3)_H$	2.81 ± 0.48	2.74 ± 0.25	2.53 ± 0.36	2.56 ± 0.20	2.83 ± 0.14
$(2)_D/(3)_D$	3.04 ± 0.08	2.79 ± 0.35	0.92 ± 0.11	0.87 ± 0.15	8.29 ± 0.13
$[(2)_H + (3)_H]/[(2)_D + (3)_D]$	0.95 ± 0.09	0.94 ± 0.05	1.17 ± 0.03	1.12 ± 0.05	0.95 ± 0.02
$[(2)_H/(3)_H]/[(2)_D/(3)_D]$	0.92 ± 0.14	0.99 ± 0.09	2.75 ± 0.11	2.99 ± 0.30	0.34 ± 0.02
Liver sample 2					
$(3)_H/(3)_D$	1.00 ± 0.03	1.02 ± 0.01	0.69 ± 0.03	0.67 ± 0.04	2.30 ± 0.14
$(2)_H/(2)_D$	0.96 ± 0.09	1.03 ± 0.04	1.72 ± 0.02	1.83 ± 0.03	0.80 ± 0.05
$(2)_H/(3)_H$	2.42 ± 0.21	2.65 ± 0.17	2.50 ± 0.18	2.50 ± 0.13	2.35 ± 0.16
$(2)_D/(3)_D$	2.55 ± 0.31	2.62 ± 0.12	1.00 ± 0.06	0.92 ± 0.03	6.77 ± 0.35
$[(2)_H + (3)_H]/[(2)_D + (3)_D]$	0.97 ± 0.07	1.02 ± 0.02	1.20 ± 0.01	1.22 ± 0.02	0.99 ± 0.03
$[(2)_H/(3)_H]/[(2)_D/(3)_D]$	0.95 ± 0.06	1.01 ± 0.04	2.51 ± 0.15	2.73 ± 0.20	0.35 ± 0.04

[$^2H_2$]-1. This is due to rapid nonenzymatic exchange of deuterium substituents in position 5 of 3 and its tautomeric 1,6-unsaturated cation 5 (16).

^{D}(V/K) for the formation of 2, a measure of the apparent kinetic isotope effect, was 2.18 ± 0.07 (± standard deviation), similar for both liver samples and for either 1 isotopomer labeled at position 2*S*, i.e., 2*S*-[^{2}H]-1 and 2,2-[$^2H_2$]-1. The corresponding ^{D}(V/K) for the formation of 3 was consistently <1 (0.64 ± 0.06). ^{D}(V/K) for total metabolism was >1 (1.33 ± 0.06).

***In vitro* experiments with internal competition between two different sparteine isotopomers.** Incubations of equimolar mixtures of regioselectively and stereoselectively labeled sparteines and 15,15,17,17-[$^2H_4$]-1 were analyzed using GC-MS as described in Materials and Methods. The amounts of the two metabolites were measured at the respective mass traces. Control experiments with 15,15,17,17-[$^2H_4$]-1 revealed no loss of deuterium in the metabolites formed; in addition, enzyme kinetic parameters showed no significant difference from the results for undeuterated 1 (Table 1). Therefore, [15,15,17,17-$^2H_4$]-1 was regarded as a suitable isotopomer to reflect the kinetic characteristics of undeuterated 1 for competitive *in vitro* and *in vivo* experiments. This finding was confirmed by incubations of an equimolar mixture of [$^2H_0$]-1 and 15,15,17,17-[$^2H_4$]-1; the amounts of [$^2H_0$]dehydrosparteine and [$^2H_4$]dehydrosparteine formed in two human liver microsome samples were not significantly different. Results of isotope effects as determined by the competitive method are listed in Table 2. Again, deuterium isotope effects were observed when 2*S*-[^{2}H]-1, 2,2-[$^2H_2$]-1, or 6-[^{2}H]-1 was used as substrate but were evidently absent with 2*R*-[^{2}H]-1.

The ratio $(2)_H/(2)_D$, which indicates the apparent kinetic isotope effect for the formation of 2, was 1.76 ± 0.05, similar for both liver samples using either 2*S*-[^{2}H]-1 or 2,2-[$^2H_2$]-1 as substrate. The ratio $(3)_H/(3)_D$ was always significantly <1, which is consistent with the results obtained in the noncompetitive experiments.

***In vivo* studies on sparteine metabolism.** Table 3 shows the results of both competitive and noncompetitive *in vivo* experiments. The degree of deuterium abstraction from 2*S*- or deuterium retention from 2*R*-[^{2}H]-1 during the formation of 2 was >95%. Apparent isotope effects determined as the ratios of the metabolites excreted in the urine by either the competitive or noncompetitive method were very similar to the results obtained *in vitro*.

Chemical oxidation of sparteine and 17-oxosparteine. When 1 was used as a substrate for various chemical or electrochemical oxidation experiments, 6 or 17-hydroxysparteine was readily formed (results not shown). Because the sparteine molecule was evidently not oxidized at N1, a substrate was used, in which N16 was less easily oxidized. This was achieved by the use of the sparteine monolactam 6. Experiments on the chemical oxidation of 6 by Ce^{4+} resulted in the formation of 7, which was identified by GC-MS. Structural confirmation was obtained by direct comparison with the synthetic compound. No other product peak was observed by GC, GC-MS, or high performance thin layer

TABLE 3

Kinetic deuterium isotope effects of *in vivo* sparteine metabolism determined by competitive and noncompetitive experiments

Sparteine metabolites were quantified by GC (noncompetitive study design) or GC-MS (competitive study design) in urine of an EM subject. Ratios $(2)_H/(2)_D$ and $(3)_H/(3)_D$ reflect apparent isotope effects comparable to $(V)_H/(V)_D$ in competitive or $(V_{max}/K_m)_H/(V_{max}/K_m)_D$ in noncompetitive *in vitro* experiments, respectively.

Method	Substrate	$(2)_H/(2)_D$[c]	$(3)_H/(3)_D$[c]
Competitive[a]	[$^2H_0$]-1	0.97	1.06
	2*R*-[^{2}H]-1	0.96	1.04
	2*S*-[^{2}H]-1	1.67	0.61
	6-[^{2}H]-1	0.88	2.67
Noncompetitive[b]	15,15,17,17-[$^2H_4$]-1	1.1	1.1
	2*R*-[^{2}H]-1	1.1	1.0
	2*S*-[^{2}H]-1	1.8	0.5
	2,2-[$^2H_2$]-1	1.9	0.5
	6-[^{2}H]-1	0.9	2.6
	5,5-[$^2H_2$]-1	1.0	1.0

[a] Metabolites were measured by GC-MS that were excreted in the urine 0–3 hr after oral intake of 50 mg of an equimolar mixture of 15,15,17,17-[$^2H_4$]-1 and either [$^2H_0$]-1, 2*R*-[^{2}H]-1, 2*S*-[^{2}H]-1, or 6-[^{2}H]-1.

[b] Metabolites excreted in the urine 0–15 hr after oral intake of the respective 1 isotopomers were quantified by GC.

[c] Competitive method: ratio of the metabolites formed from the differently labeled 1 compared with the metabolites of 15,15,17,17-[$^2H_4$]-1.

Noncompetitive method: ratio of the amounts of metabolites excreted in the urine compared with unlabeled 1.

chromatography analysis. In a typical experiment, ~30% of **6** was converted to **7**. No significant isotope effect (0.99 ± 0.05 [± standard deviation], six experiments) was observed with the unlabeled **6** compared with 15,15-[$^2H_2$]-**6**, indicating that 15,15-[$^2H_2$]-**6** can be used as internal reference compound for the competitive experimental approach. With 6-[^{2}H]-**6**, an isotope effect of 1.21 ± 0.1 (six experiments) was found for the formation of **7**. GC or GC-MS analysis of *in vitro* experiments on microsomal metabolism of **6** revealed no metabolism by human liver microsomes.

Discussion

Recently, Gillette *et al.* published a theory that distinguishes the three possible kinetic mechanisms for the P450-catalyzed oxidation of a substrate that is converted into at least two different products by a single isoform (12, 13). The theory relies on a comparison of competitive and noncompetitive deuterium isotope effects at the metabolic site in the substrate that does not involve the loss of deuterium on oxidation.

The theory of Gillette *et al.* states that (a) a parallel pathway mechanism, i.e., one that has a fixed orientation of the substrate in the active site of the enzyme, will have a value of 1.0 for both $(v)_H/(v)_D$ in the competitive experiment and $(V_{max}/K_m)_H/(V_{max}/K_m)_D$ in the noncompetitive experiment; (b) the dissociative mechanism, i.e., one in which the substrate can both dissociate and reassociate with the active site in different orientations before catalysis, producing different activated EOS complexes, will have a value of 1.0 for $(v)_H/(v)_D$ in the competitive experiment but a value of <1.0 to >1.0 for $(V_{max}/K_m)_H/(V_{max}/K_m)_D$ in the noncompetitive experiment; and (c) the nondissociative mechanism, i.e., one that allows changes in the orientation of the bound substrate to form different EOS complexes without dissociation of the substrate from the activated enzyme, will have a value of <1.0 for both $(v)_H/(v)_D$ in the competitive experiment and $(V_{max}/K_m)_H/(V_{max}/K_m)_D$ in the noncompetitive experiment.

In our *in vitro* and *in vivo* studies with 2*S*-[^{2}H]-**1** or 2,2-[$^2H_2$]-**1**, isotope effects of <1.0 for the formation of **3**, the metabolite that is formed without loss of deuterium, were observed in both competitive and noncompetitive experiments. Therefore, CYP2D6-catalyzed **1** metabolism proceeds via a nondissociative mechanism (Fig. 3). In addition, isotope effects on total metabolism in noncompetitive [Table 1; $^D(V/K)_{tot.}$] and competitive (Table 2; ratio of sums of metabolites) experiments were significantly >1.0 with the substrate 2*S*-[^{2}H]-**1** or 2,2-[$^2H_2$]-**1**. According to the theory for nondissociative kinetic mechanisms, this observation is probably due to the unproductive reduction of the EOS_W complexes to form the respective ES_W complexes and water rather than continuing to **2** and **3** product formation.

When 6-[^{2}H]-**1** was used as substrate in either competitive and noncompetitive experiments, normal isotope effects, i.e., >1.0, were observed for the formation of the deuterium sensitive metabolite **3**, and inverse isotope effects were found for **2**, again indicating a nondissociative kinetic mechanism. In contrast to the results with 2*S*-[^{2}H]-**1** or 2,2-[$^2H_2$]-**1**, isotope effects on total metabolism were not significantly different from 1.0, suggesting no detectable reduction of the EOS complexes to water.

Thus, the sparteine molecule that is bound to the substrate binding pocket of CYP2D6 is able to perform some orientational changes resulting in kinetically distinguishable EOS complexes via a nondissociative mechanism. The presence of this nondissociative mechanism might indicate that the binding forces by ionic interaction of the positively charged N16 of **1**, or corresponding functional groups of other CYP2D6 substrates, and the substrate binding carboxylate group of CYP2D6 are relatively strong.

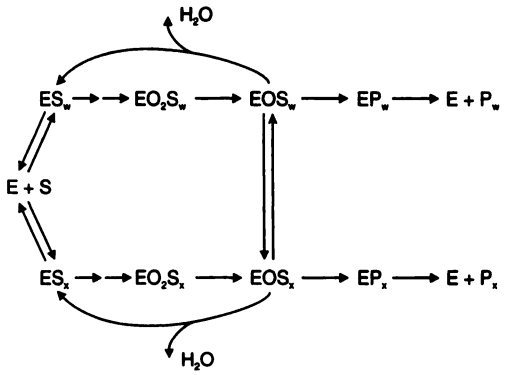

Fig. 3. Nondissociative kinetic mechanism according to Gillette *et al.* (12) for the formation of two different metabolites by P450. Regarding 2*S*-[^{2}H]-**1** as an example of a substrate isotopomer, *subscript W*, which indicates a deuterium abstraction metabolic pathway, stands for the formation of the major human metabolite **4** and its intermediates. Accordingly, *subscript X* denotes the deuterium-insensitive metabolic reaction. With 2*S*-[^{2}H]-**1** as an example, this is the formation of the human minor metabolite and its intermediates, i.e., P_x in this case is **3**. Other abbreviations are as in Ref. 12: *E*, enzyme; *ES*, enzyme/substrate complex; EO_2S, dioxygenated enzyme/substrate complex; *EOS*, activated enzyme substrate/complex (after cleavage of the oxygen-oxygen bond and release of water); *EP*, enzyme/product complex.

In branched reaction pathways, the ratio of the product ratios of the unlabeled and the deuterium containing substrate in competitive experiments or the ratio of the ratio of the rates of metabolite formation from the unlabeled or deuterated substrate approach the intrinsic isotope effect (25–27) provided that the rates of interconversion of the different activated EOS complexes are fast relative to bond breaking (rapidly interconvertible branched chain mechanism).

Application of this method to human sparteine metabolism revealed similar results for human metabolites both *in vitro* and *in vivo*. Depending on the experimental design, which was either competitive or noncompetitive, intrinsic kinetic deuterium isotope effects were found in the range of 2.9–3.8 or 2.5–3.0, respectively. Because isotope effects on the respective metabolic pathway that does not require deuterium abstraction were clearly <1 in all experiments, the rates at which the activated EOS complexes interconvert appear to be fast relative to the rate of formation of the EP complex or the rate of reduction to water and ES (27). However, the rate constant for EOS interconversion is probably not sufficiently large to allow full expression of the intrinsic isotope effect, and therefore the intrinsic kinetic deuterium isotope effects of 2.5–3.8 should be regarded as representing the lower limit for the true intrinsic isotope effect.

The purpose of calculating intrinsic isotope effects on enzyme-catalyzed reactions has been to gain knowledge of the geometry of the transition state, which is the core of the reaction mechanism for metabolite formation. Thus, kinetic isotope effects have often been used to distinguish between different mechanisms of P450-catalyzed *N*-dealkylation reac-

tions. The approach is based on the assumption that aminium radical deprotonation is fast, does not contribute significantly to the overall reaction rate, and therefore will result in low kinetic isotope effects. Isotope effects of ≤3.6 have been regarded as criteria for aminium radical cation mechanisms, whereas initial hydrogen abstraction is believed to be associated with isotope effects of >7 (11).

According to this approach, our results would be interpreted in favor of the initial nitrogen oxidation pathway A. However, two aspects must be taken into account for the interpretation of such results on deprotonation reactions: the acidity of the cation radical C(α)—H bonds and the basicity of bases present in the reaction mixture that serve as proton acceptors.

Acidities of α-hydrogens of aminium radical cations have been found to be unexpectedly low (28). Consequently, deprotonation reactions of stable aromatic cation radicals exhibit exceptionally large deuterium isotope effects ranging from 3.6 to 22 (29, 30), and substantial differences for the rate constants of deprotonation reactions were observed using different bases, e.g., pyridine or acetate, as proton acceptors. Accordingly, the smaller deuterium isotope effect of 1.21, measured for chemical oxidation of 17-oxosparteine to the 5,6-unsaturated enamine by the one-electron oxidant Ce^{4+}, cannot be interpreted as proof of a reaction mechanism via initial aminium radical cation formation.

In addition, there is evidence that reaction mechanisms proceeding by initial hydrogen abstraction at the α-carbon of amines can result in kinetic deuterium isotope effects of ≤3.6 (31).

Thus, it seems that a clear discrimination between mechanisms A and B is difficult to achieve by means of the magnitude of kinetic deuterium isotope effects, and therefore other parameters, such as regiospecificity and stereospecificity of metabolite formation, should be considered.

Unlike chemical or electrochemical oxidation, CYP2D6-mediated metabolism of **1** takes place at ring A of the sparteine molecule exclusively. Two metabolites are formed by human *in vitro* or *in vivo* metabolism at an essentially constant **2**/**3** ratio of ~0.2 (31a). With no **3** detectable in rats, sparteine oxidation shows pronounced species differences (9, 32). Our results also indicate a marked stereoselectivity for the formation of **2**, i.e., hydrogen/deuterium is selectively abstracted from the β side. Similar results were obtained for **2** formation by rats *in vitro* and *in vivo* (9). In addition, metabolism of pachycarpine, the (+)-enantiomer of **1**, by the rat orthologue P450 enzyme CYP2D1 stereoselectively results in the formation of (4*S*)-hydroxypachycarpine (9). This stable aliphatic alcohol is formed by stereospecific hydroxylation of the 4β position of pachycarpine.

All of these results indicate that **1** must be orientated in the active site of both CYP2D6 and CYP2D1, such that only the β side of ring A is available for oxidative attack.

It is generally assumed that substrate binding of CYP2D6 substrates takes place by interaction of a basic nitrogen atom, i.e., N16 of **1**, and a negatively charged carboxylate group of the enzyme protein (4, 5). The intramolecular distance between the site of attack and the basic nitrogen atom has been reported to be in the range of 4.5–8 Å. Sparteine is a strongly basic compound with a pK_{a1} of 11.4 (21). ^1H and ^{13}C NMR studies revealed a stable all-chair conformation for **1** in aqueous solution at pH 5.0–10.0 (7) (Fig. 4). This all-chair monoprotonated conformation of **1** was also used as the starting structure for basic computerized molecular modeling. A value of 2.8 Å was calculated for the distance between N1 and N16, a result that agrees with the distance of 2.9 Å calculated from crystallographic data (4). Thus, the N1-to-N16 distance of the monoprotonated cage-structured sparteinium monocation appears to be too short for initial nitrogen oxidation of N1 based on the CYP2D6 pharmacophore model. Even if conformational reorientation to a ring C boat conformation occurs on fixation of **1** at the CYP2D6 substrate binding site because of interaction of the carboxylate group with N16, the distance between N1 and N16 (~3.5 Å) is still too short. However, in this conformation, which is plausible as it has been shown to also be adopted by the diprotonated sparteinium dication at pH <6, the respective distances between N16 and C2 or C6 are 5.0 and 3.6 Å. Therefore, enzymatic attack at C2 of the sparteine molecule with ring C in the boat conformation is within the range of CYP2D6 substrates.

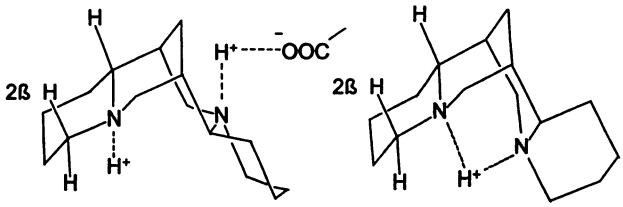

Fig. 4. Possible conformations of **1** in aqueous solutions. *Right*, all-chair conformation of the sparteinium monocation at pH 5–10. *Left*, conformation of the sparteinium dication at pH <5. Ring C adopts boat configuration together with the hypothetical substrate binding by interaction of positively charged N16 with a CYP2D6 carboxylate group.

Although these model considerations are consistent with an initial carbon radical formation, one-electron oxidation of N1 cannot be ruled out on the basis of the short distances between N1 and N16 because electron transfer from free tertiary amines to the $(Fe{=}O)^{3+}$ species of P450s is not subject to the same distance constraints as hydrogen abstraction from a carbon atom. According to calculations with substituted *N*-dimethyl anilines (33) or observations with deprenyl (34), P450-mediated electron transfers may occur over a distance of 5 Å. However, it should be kept in mind that such spatial electron transfers require the presence of the free unprotonated amine species and have been discussed for compounds with a much lower basicity than N1 of **1**.

As reported previously (4), modeling C2 attack into the molecular template of CYP2D6 substrates leads to an orientation of the sparteine molecule in which rings A and B lie almost parallel to the heme moiety of the enzyme that is located on the β side of the sparteine molecule. Therefore, our results for stereoselective abstraction of hydrogen from the β side of ring A during formation of **2** confirm the direct interaction of the enzyme with C2 of the sparteine molecule. Formation of **3** by enzymatic attack at C6 does not fit in the model for CYP2D6 substrates in either sparteine configuration. This problem has been circumvented by proposing a possible involvement of C5 during **3** formation (4). Our results, however, indicate no isotope effect with 5,5-[$^2H_2$]-**1** either *in vitro* or *in vivo*, and therefore oxidation of C5 as primary reaction resulting in the formation of **3** can be ruled out. On the other hand, if interaction of the heme-bound

oxo-iron species with the hydrogen atom to be abstracted is the first step in carbon radical formation (35), the hydrogen substituent of C6, which is also located on the β side of ring A, exhibits a distance to N16 of 4.5 Å and thus fits into the range of CYP2D6 substrates.

In contrast to P450-catalyzed **1** oxidation, the sole product of chemical oxidation of ring A of 17-oxosparteine is the 5,6-unsaturated product and therefore markedly differs from P450-catalyzed oxidation of ring A of sparteine in all species investigated.

This indicates that loss of the C6 proton from the aminium radical cation is energetically favored over loss of the C2 proton. Thus, abstraction of the C2 proton, which is favored by the enzyme over the C6 proton, requires that the enzyme compensates for the inherent energy difference by having some base that is preferentially orientated for attacking the C2 proton specifically. It has been proposed that the $(Fe \cdot O)^{2+}$ entity of the P450 itself acts as a specific base, which determines regioselectivity and stereoselectivity of product formation by selective proton abstraction from the aminium radical cation (36). However, the lone electron pair of N1 in both **1** conformations is on the opposite side from proton abstraction and thus requires reorientation and/or conformational alterations of ring A of the aminium radical cation. If these changes can occur, protons should not be exclusively abstracted from the β side, and it is also uncertain whether the aminium radical of **1**, an aliphatic amine, is stable long enough to allow such reorientations. The finding of increased nonproductive water formation during formation of **2**, but not **3**, also indicates that the two different EOS complexes are energetically or kinetically different before undergoing the first irreversible reaction step.

Therefore, instead of a "postabstraction" (12) mechanism involving reorientation of the initially formed aminium radical cation, a "preabstraction" mechanism seems more likely. Although a sequential electron-proton transfer reaction during sparteine metabolism cannot be ruled out completely, our data suggest the presence of such a preabstraction mechanism and that the sparteine metabolites are formed by direct carbon oxidation.

To our knowledge, this is the first report of *in vitro* and *in vivo* experiments using kinetic deuterium isotope effects in competitive and noncompetitive experimental designs. It clearly shows that valid predictions of *in vivo* results can be made from *in vitro* experiments. Together with previous results (13, 27), the results of the present study also show that kinetic isotope effects are still a useful tool with which to elucidate enzymatic reaction mechanisms and enzyme-substrate interactions, even though the sole use of interpretation of their magnitude to distinguish between different enzymatic reaction mechanisms is probably no longer applicable.

Acknowledgments

We are grateful to Dr. W. Trager for helpful discussions and critical reading of the manuscript.

References

1. Renumbered in proof.
2. Renumbered in proof.
3. Korzekwa, K. R., and J. P. Jones. Predicting the cytochrome P450 mediated metabolism of xenobiotics. *Pharmacogenetics* **3**:1–18 (1993).
4. Islam, S. A., C. R. Wolf, M. S. Lennard, and M. J. E. Sternberg. A three-dimensional molecular template for substrates of human cytochrome P450 involved in debrisoquine 4-hydroxylation. *Carcinogenesis* **12**:2211–2219 (1991).
5. Koymans, L., N. P. E. Vermeulen, S. A. B. E. van Acker, J. M. te Koppele, J. J. P. Heykants, K. Lavrijsen, W. Meuldermans, and G. M. Donné-Op den Kelder. A predictive model for substrates of cytochrome P450-debrisoquine (2D6). *Chem. Res. Toxicol.* **5**:211–219 (1992).
6. Strobl, G. R., S. Vonkruedener, J. Stockigt, F. P. Guengerich, and T. Wolff. Development of a pharmacophore for inhibition of human liver cytochrome P-450 2D6: molecular modeling and inhibition studies. *J. Med. Chem.* **36**:1136–1145 (1993).
7. Schneider, F., P. Fischer, T. Ebner, and C. O. Meese. Conformation of the CYP2D6 model substrate sparteine under physiological conditions. *Bioorg. Med. Chem. Lett.* **3**:1667–1670 (1993).
8. Guengerich, F. Oxidation of sparteine by cytochrome P-450: evidence against the formation of N-oxides. *J. Med. Chem.* **27**:101–1103 (1984).
9. Ebner, T., C. O. Meese, and M. Eichelbaum. Regioselectivity and stereoselectivity of the metabolism of the chiral quinolizidine alkaloids sparteine and pachycarpine in the rat. *Xenobiotica* **21**:847–857 (1991).
10. Miwa, G. T., W. A. Garland, B. J. Hodshon, A. Y. H. Lu, and D. B. Northrop. Kinetic isotope effects in cytochrome P-450-catalyzed oxidation reactions. *J. Biol. Chem.* **255**:6049–6054 (1980).
11. Miwa, G. T., J. S. Walsh, G. L. Kedderis, and P. F. Hollenberg. The use of intramolecular isotope effects to distinguish between deprotonation and hydrogen atom abstraction mechanisms in cytochrome P-450- and peroxidase-catalyzed N-demethylation reactions. *J. Biol. Chem.* **258**:14445–14449 (1983).
12. Gillette, J. R., J. F. Darbyshire, and K. Sugiyama. Theory for the observed isotope effect on the formation of multiple products by different kinetic mechanisms of cytochrome P450 enzymes. *Biochemistry* **33**:2927–2937 (1994).
13. Darbyshire, J. F., J. R. Gillette, K. Nagata, and K. Sugiyama. Deuterium isotope effects on A-ring and D-ring metabolism of testosterone by CYP2C11: evidence for dissociation of activated enzyme-substrate complexes. *Biochemistry* **33**:2938–2944 (1994).
14. Ebner, T., J. Rebell, P. Fischer, and C. O. Meese. Synthesis and spectroscopic stereospecificity assay of the deuterated quinolizidine alkaloids 2*S*-[^{2}H]- and 2*R*-[^{2}H]-sparteine. *J. Labelled Compd. Radiopharm.* **27**:485–489 (1989).
15. Golebiewski, W. M., and I. D. Spenser. Lactams of sparteine. *Can. J. Chem.* **63**:716–719 (1985).
16. Meese, C. O., and T. Ebner. Synthesis of 5-, 6-, and 7-deutero sparteines. *J. Labelled Compd. Radiopharm.* **25**:329–334 (1988).
17. Bohlmann, F. Zur Konfigurationsbestimmung von Chinolizidin-Derivaten. *Chem. Ber.* **91**:2157–2167 (1958).
18. Rink, M., and K. Grabowski. Zur Kenntnis des 17-Hydroxylsparteins. *Arch. Pharm.* **289**:695–702 (1956).
19. Ebner, T., H. Lackner, G. Remberg, and C. O. Meese. 2,3-Didehydrospartein. *Liebigs Ann. Chem.* 197–201 (1989).
20. Leonard, N. J., P. D. Thomas, and V. W. Gash. Structures and reactions of the dehydrosparteines and their salts. *J. Am. Chem. Soc.* **77**:1552–1558 (1955).
21. Dayer, P., R. Gasser, J. Gut, T. Kronbach, G. M. Robertz, M. Eichelbaum, and U. A. Meyer. Characterization of a common genetic defect of cytochrome P-450 function (debrisoquine-sparteine type polymorphism): increased Michaelis constant (Km) and loss of stereoselectivity of bufuralol 1′-hydroxylation in poor metabolizers. *Biochem. Biophys. Res. Commun.* **125**:374–380 (1984).
22. Osikowska-Evers, B. A., and M. Eichelbaum. A sensitive capillary GC assay for the determination of sparteine oxidation products in microsomal fractions of human liver. *Life Sci.* **38**:1775–1782 (1986).
22a. Ebner, T., C. O. Meese, P. Fischer, and M. A. Eichelbaum. Nuclear magnetic resonance study of sparteine *delta* metabolite structure. *Drug Metab. Dispos.* **19**:955–959 (1991).
23. Northrop, D. B. Determining the absolute magnitude of hydrogen isotope effects, in *Isotope Effects on Enzyme-Catalyzed Reactions*. (W. W. Cleland, M. H. O'Leary, and D. B. Northrop, eds.). University Park Press, Baltimore/London/Tokyo, 122–151 (1977).
24. Northrop, D. B. The expression of isotope effects on enzyme-catalyzed reactions. *Ann. Rev. Biochem.* **50**:103–131 (1981).
25. Jones, J. P., K. R. Korzekwa, A. E. Rettie, and W. F. Trager. Isotopically sensitive branching and its effect on the observed intramolecular isotope effects in cytochrome P-450 catalyzed reactions: a new method for the estimation of intrinsic isotope effects. *J. Am. Chem. Soc.* **108**:7074–7078 (1986).
26. Korzekwa, K. R., W. F. Trager, and J. R. Gillette. Theory for the observed isotope effects from enzymatic systems that form multiple products via branched reaction pathways: cytochrome P-450. *Biochemistry* **28**:9012–9018 (1989).
27. Korzekwa, K. R., W. F. Trager, K. Nagata, A. Parkinson, and J. R. Gillette. Isotope effect studies on the mechanism of the cytochrome P-450IIA1-catalyzed formation of delta-6-testosterone from testosterone. *Drug Metab. Dispos.* **18**:974–979 (1990).
28. Nelsen, S. F., and J. T. Ippoliti. On the deprotonation of trialkylamine cation radicals by amines. *J. Am. Chem. Soc.* **108**:4879–4881 (1986).

29. Dinnocenzo, J. P., and T. E. Banach. Deprotonation of tertiary amine cation radicals: a direct experimental approach. *J. Am. Chem. Soc.* **111:** 8646–8653 (1989).
30. Parker, V. D., and M. Tilset. Facile proton transfer reactions of N,N-dimethylaniline cation radicals. *J. Am. Chem. Soc.* **113:**8778–8781 (1991).
31. Dinnocenzo, J. P., S. B. Karki, and J. P. Jones. On isotope effects for the cytochrome P-450 oxidation of substituted N,N-dimethylanilines. *J. Am. Chem. Soc.* **115:**7111–7116 (1993).
31a. Eichelbaum, M., K. P. Reetz, E. K. Schmidt, and C. Zekorn. The genetic polymorphism of sparteine metabolism. *Xenobiotica* **16:**465–481 (1986).
32. Otton, S. V., R. F. Tyndale, D. Wu, T. Inaba, W. Kalow, and E. M. Sellers. Catalytic and immunologic similarities between monkey and human liver cytochrome P-450db1 (human cytochrome P-450 2D6). *Drug Metab. Dispos.* **20:**1–5 (1992).
33. Macdonald, T. L., W. G. Gutheim, R. B. Martin, and F. P. Guengerich. Oxidation of substituted N,N-dimethylanilines by cytochrome P-450: estimation of the effective oxidation-reduction potential of cytochrome P-450. *Biochemistry* **28:**2071–2077 (1989).
34. Grace, J. M., M. T. Kinter, and T. L. Macdonald. Atypical metabolism of deprenyl and its enantiomer, (*S*)-(+)-N,α-dimethyl-N-propynylphenethylamine, by cytochrome P450 2D6. *Chem. Res. Toxicol.* **7:**286–290 (1994).
35. White, R. E., and M. J. Coon. Oxygen activation by cytochrome P-450. *Ann. Rev. Biochem.* **49:**315–356 (1980).
36. Okazaki, O., and F. P. Guengerich. Evidence for specific base catalysis in N-dealkylation reactions catalyzed by cytochrome P450 and chloroperoxidase. *J. Biol. Chem.* **268:**1546–1552 (1993).

Send reprint requests to: Dr. Thomas Ebner, Dr. Karl Thomae GmbH, Department of Pharmacokinetics and Drug Metabolism, Birkendorfer Str. 65, D-88397 Biberach, Germany.